Springer

Journal of
Mechanical
Science and
Technology

Journal of Mechanical Science and Technology 23 (2009) 3448~3458

www.springerlink.com/content/1738-494x
DOI 10.1007/s12206-009-1018-8

Approximate method of determining the optimum cross section of microhannel heat sink †

Omid Asgari* and Mohammad Hassan Saidi

Department of Mechanical Engineering, Sharif University of Technology, Tehran, 11365-9567, Iran

(Manuscript Received May 13, 2009; Revised July 14, 2009; Accepted August 1, 2009)

Abstract

Microchannels are at the forefront of today's cooling technologies. They are widely being considered for cooling of electronic devices and in micro heat exchanger systems due to their ease of manufacture. One issue which arises in the use of microchannels is related to the small length scale of the channel or channel cross-section. In this work, the maximum heat transfer and the optimum geometry for a given pressure loss have been calculated for forced convective heat transfer in microchannels of various cross-section having finite volume for laminar flow conditions. Solutions are presented for 10 different channel cross sections: parallel plate channel, circular duct, rectangular channel, elliptical duct, polygonal duct, equilateral triangular duct, isosceles triangular duct, right triangular duct, rhombic duct and trapezoidal duct. The model is only a function of the Prandtl number and the geometrical parameters of the cross-section, i.e., area and perimeter. This solution is performed with two exact and approximate methods. Finally, in addition to comparison and discussion of these two methods, validation of the relationship is provided using results from the open literature.

Keywords: Microchannels; Optimization; Constructal; Laminar flow; Convective heat transfer; Exact and approximate methods

1. Introduction

The cooling of high-power electronic devices requires renewed attention as power dissipation from electronic components continues to increase. Reflecting the trends in electrical microcircuits, the size of cooling systems must decrease while power dissipation increases. Although many different techniques could potentially provide adequate cooling, small-scale channels embedded in a solid substrate offer particular promise due to their small sizes and high rates of heat transfer.

Tuckerman and Pease [1] were the first to demonstrate that planar integrated circuit chips can be effectively cooled by laminar water flowing through microchannels with hydraulic diameters of 86 to 95 μm [2]. That is, as the characteristic length scale of the cross-section becomes smaller and smaller, the propensity for fully developed laminar flow increases. Since the heat transfer coefficient diminishes with increasing flow length, as does the heat transfer effectiveness of the fluid, it is desirable to maximize heat transfer for a fixed volume and mean system temperature.

This issue can be addressed by considering the elemental passage geometries and determining the best passage size and configuration for a fixed volume, which is to be convectively cooled with a fluid stream supplied at constant pressure drop. Bejan and Sciubba [3] first considered this problem for an array of parallel plates with application to the cooling of electronic systems. Using the intersection of asymptotes method, Bejan and Sciubba [3] obtained expres-

† This paper was recommended for publication in revised form by Associate Editor Jae Dong Chung

*Corresponding author. Tel.: +98 9126779749, Fax.: +98 2166000021
E-mail address: o_asgari@mech.sharif.edu

sions for the optimal plate spacing to channel length ratio and the maximum heat transfer per unit volume in terms of a dimensionless parameter which is now referred to as the Bejan number [4].

Yilmaz et al. [5] applied an exact method of analysis to obtain results for a single duct for the equilateral triangle, square, circular, and parallel plate geometries.

In the present work, the approximate analysis method of Bejan and Sciubba [3] and exact analysis method of Yilmaz et al. [5] are applied to several other channel shapes to determine the optimal channel size to length ratio and the maximum heat transfer in terms of the Bejan number.

2. Asymptotic or approximate analysis

Considering the geometry that contains an array of circular or non-circular passages. In this simple analysis the flow is assumed laminar, the board temperature and the flow distribution is assumed to be uniform. The pressure head established by the pump, ΔP, is fixed; there are other assumptions such as constant cross-sectional duct area, Prandtl number range $Pr>0.1$, and a finite control volume ($V=HWL$). The method consists of two steps. In the first, we identify the two possible extremes: the small ducts or channels and the large ducts or channels. In the second step, the two extremes are intersected to determine the optimum size of channels that maximizes heat transfer.

2.1 Small channels (With small characteristic length)

When characteristic length becomes sufficiently small, it could be assumed that flow and heat transfer are fully developed. In this limit, the mean outlet temperature of the fluid approaches the board temperature, $T_w=T_{max}$. The total rate of heat transfer from the first law of thermodynamics is [3]

$$\dot{Q}_a = \dot{m} C_p \left(T_w - T_i\right) \tag{1}$$

where T_i is the inlet temperature. The mass flow rate is

$$\dot{m} = \rho UHW = \rho UnA_r \tag{2}$$

where A_r is the reference cross sectional area of an elemental channel as shown in Fig. 1 for a typical duct, and n is the total number of channels. For the case of rectangular, square and triangular ducts which are fully packed, $A=A_r$.

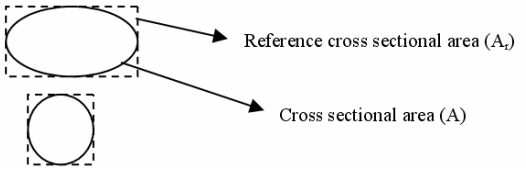

Fig. 1. Difference between A and A_r.

The mean velocity, U, in duct or channel, may be determined from the pressure drop of fully developed and laminar flow [6, 7] defined as

$$U = (\Delta P D_h^{\,2}) \Big/ (2 f \,\mathrm{Re}_{D_h} L\mu) \tag{3}$$

Combining the above mentioned three equations gives the heat transfer rate in terms of the basic flow variables

$$\dot{Q}_a = \rho HW \frac{\Delta P D_h^{\,2}}{2 f \,\mathrm{Re}_{D_h} L\mu} C_p \left(T_w - T_i\right) \tag{4}$$

The above equation may be written in the following form:

$$\dot{Q}_a = \frac{\rho \Delta P C_p \left(T_w - T_i\right)}{\mu} \frac{HW}{2 f \,\mathrm{Re}_{D_h} L} D_h^{\,2} = CaD_h^2 \tag{5}$$

The $f\mathrm{Re}_{Dh}$ is reported for some different configurations in Shah and London [8] and Kakac, Shah and Aung [9], where D_h is defined as $D_h= 4A/P$. Considering that Ca is constant, it can easily be shown that the heat transfer rate has the following dependency:

$$\dot{Q}_a \sim D_h^2 \tag{6}$$

This trend is illustrated by the small D_h asymptote in Fig. 2.

2.2 Large channels (With large characteristic length)

Considering the limit in which channel dimensions are large enough that they exceed the thickness of the thermal boundary layer that forms on each surface. In this case it is necessary to determine the free-stream velocity U_∞ that sweeps these boundary layers. Since the pressure drop ΔP is fixed, a force balance on the

$H \times L \times W$ control volume reads [3]

$$\Delta PHW = \bar{\tau}\, pnL \tag{7}$$

where $\bar{\tau}$ is the wall shear stress averaged over L in laminar flow given as [7]

$$\bar{\tau} = 0.664 \rho U_\infty{}^2 \,\mathrm{Re}_L{}^{-1/2} \quad \left(\mathrm{Re}_L = U_\infty L/\nu \le 5\times 10^5\right) \tag{8}$$

Combining Eqs. (7) and (8) gives the below result for U_∞

$$U_\infty = \left(\Delta PHW / 0.664 \rho L^{0.5} \nu^{0.5} pn\right)^{2/3} \tag{9}$$

The heat transfer rate through a large channel (that is within entrance length) is

$$\dot{Q}_l = \bar{h} A_s \left(T_w - T_i\right) = \bar{h} pL \left(T_w - T_i\right) \tag{10}$$

where $\bar{h}$ is the heat transfer coefficient averaged over L, that may be defined from the expression for laminar boundary layer flow over a flat plate [7]:

$$\bar{h}L/k = 0.664\,\mathrm{Pr}^{1/3}\,\mathrm{Re}_L{}^{1/2} \quad \left(\mathrm{Re}_L \le 5\times 10^5 \quad \mathrm{Pr} \ge 0.5\right) \tag{11}$$

The total heat transfer rate from the entire package is

$$\dot{Q}_b = 0.761 \frac{k\,\mathrm{Pr}^{1/3}\,\Delta P^{1/3}\left(T_w - T_i\right)}{\rho^{1/3} \upsilon^{2/3}} \left(n^2 LHW p^2\right)^{1/3} = Cb\left(n^2 p^2\right)^{1/3} \tag{12}$$

Considering $n = HW/A_r$, $A_r \sim D_h{}^2$ and $p \sim D_h$, the total heat transfer rate varies as

$$\dot{Q}_b \sim D_h^{-2/3} \tag{13}$$

This trend is shown in Fig. 2.

2.3 Optimum channel size

The optimal channel size may be found by means of the method of intersecting asymptotes [6, 7]. However, the intersection point of the two asymptotic

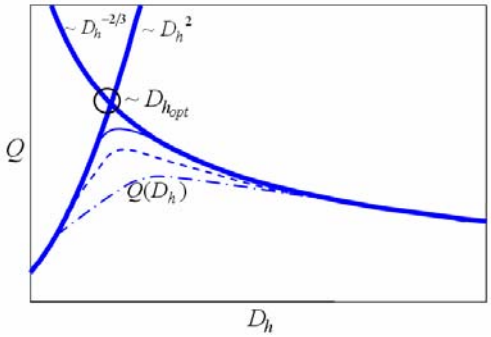

Fig. 2. Method of intersecting asymptotes.

results is relatively close to the exact point. Intersecting Eqs. (5) and (12) ($\dot{Q}_a = \dot{Q}_b$) gives [3]

$$\frac{\rho \Delta P C_p \left(T_w - T_i\right)}{\mu} \frac{HWD_h{}^2}{2 f\,\mathrm{Re}_{D_h} L} \approx 0.761 \frac{k\,\mathrm{Pr}^{1/3}\,\Delta P^{1/3}\left(T_w - T_i\right)}{\rho^{1/3}\nu^{2/3}} \left(n^2 LHW\, p^2\right)^{1/3} \tag{14}$$

After simplifying and collecting the system and geometry terms, i.e., $n=HW/A_r$, $Pr=\nu/\alpha$, $\alpha=k/\rho C_p$, $\nu=\mu/\rho$, the above equation may be written in the following form:

$$\left(\frac{\Delta PL^2}{\mu\alpha}\right)^{2/3} = \frac{1.52\, L^{8/3}}{(Ar/p)^{2/3}\left(D_h{}^2/f\,\mathrm{Re}_{D_h}\right)} \tag{15}$$

where $Be=\Delta PL^2/\mu\alpha$ is the Bejan number as defined in [4]. The right hand side is only a function of the duct shape and aspect ratio, while the left hand side is a system parameter which is constant and independent of duct shape or aspect ratio. When the hydraulic diameter is chosen, $D_h=4A/p$, the optimal solution is determined by solving

$$\left(Be\right)^{2/3} = 0.095\, f\,\mathrm{Re}_{D_h} \left(pL/A\right)^2 \left(pL/A_r\right)^{2/3} \tag{16}$$

2.4 Maximum heat transfer

Heat transfer per unit volume for small channels (Eq. (5)), considering $D_h=4A/p$ is given by [3]

$$\dot{q} = \frac{\dot{Q}_a}{HWL} = kBe\left(T_{\max} - T_i\right) \frac{8}{f\,\mathrm{Re}_{D_h} L^2} \left(\frac{pL}{A}\right)^{-2} \tag{17}$$

The maximum heat transfer rate per unit volume for a fixed volume can be obtained from Eq. (17) using the optimal result determined by Eq. (16). Substituting $(pL/A)^{-2}$ from Equation (16) in Eq. (17) we have

$$\dot{q}_{\max} = 0.761\, k\left(T_{\max} - T_i\right) Be^{1/3} \left(p/A_r\right)^{2/3} L^{-4/3} \quad (18)$$

The maximum dimensionless heat transfer rate per unit volume is given by

$$Q^*_{\max} = \left(\dot{q}_{\max} L^2\right) / k\left(T_{\max} - T_i\right) \quad (19)$$

or

$$Q^*_{\max} = [0.761 \quad (pL/A_r)^{2/3}] Be^{1/3} \quad (20)$$

2.5 Investigation of different geometries

We may now consider several common geometries as shown in Fig. 3.

The geometric parameters that are required in the general analysis listed in Table 1, in which A, A_r, p and D_h, are cross sectional area, reference cross sectional area, perimeter and hydraulic diameter of an elemental channel, respectively.

The product of Reynolds number and Fanning friction factor [8, 9], fRe, of fully developed laminar flow for various cross-sections, in which characteristic length is hydraulic diameter (D_h), listed in Table 2.

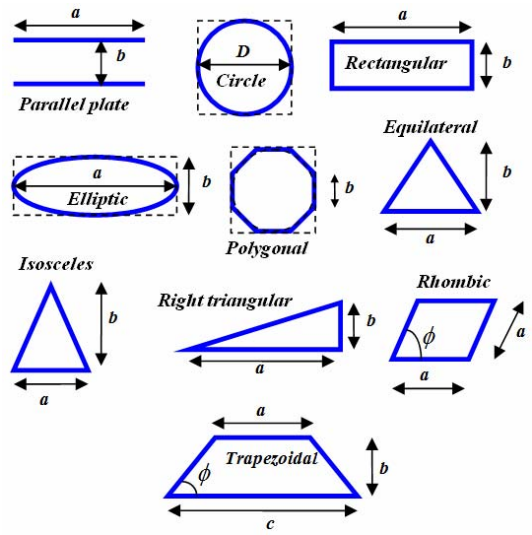

Fig. 3. Different cross sectional area.

In this table the fRe values for Trapezoidal channel, $f(\alpha^*, \Phi)$, are tabulated in Shah [10]. Substituting the results of Tables 1 and 2 into Eq. (16) and so combining it with Eq. (20) gives the following result for the optimal size of channel, b_{opt}/L, and maximum dimensionless total heat transfer rate per unit volume, Q^*_{max}, respectively.

For parallel plate channel

$$b_{opt}/L = 2.725\, Be^{-1/4} \quad (21a)$$

$$Q^*_{\max} = 0.619\, Be^{1/2} \quad (21b)$$

Table 1. Geometric parameters for various cross sections.

Parallel plate	$A=ab$	Circular duct	$A=\pi D^2/4$
	$A_r=ab$		$A_r=D^2$
	$p=2a$		$p=\pi D$
	$D_h=2b$		$D_h=D$
Rectangular channel	$A=ab$	Elliptical channel	$A=\pi ab/4$
	$A_r=ab$		$A_r=ab$
	$p=2(a+b)$		$p=2aE(m)$
	$D_h=2ab/(a+b)$		$D_h=\pi b/2E(m)$
Rhombic channel	$A=ab=a^2\sin\Phi$	Equilateral triangular channel	$A=0.5ab$
	$A_r=ab=a^2\sin\Phi$		$A_r=0.5ab$
	$p=4a$		$p=3a$
	$D_h=a\sin\Phi=b$		$D_h=2b/3$
Polygonal channel	$A=(nb^2/4)\cot(\pi/n)$		
	$A_r=d_c^2=b^2/\sin^2(\pi/n)$		
	$p=nb$		
	$D_h=b\cot(\pi/n)=d_c^{[*]}\cos(\pi/n)$		
Isosceles triangular channel	$A=0.5ab$		
	$A_r=0.5ab$		
	$p=a+\sqrt{a^2+4b^2}$		
	$D_h=(2ab)/(a+\sqrt{a^2+4b^2})$		
Right triangular channel	$A=0.5ab$		
	$A_r=0.5ab$		
	$p=a+b+\sqrt{a^2+b^2}$		
	$D_h=(2ab)/(a+b+\sqrt{a^2+b^2})$		
Trapezoidal channel	$A=0.5b\,(a+c^{[**]})$		
	$A_r=0.5b\,(a+c)$		
	$p=(a+c)+2(b/\sin\Phi)$		
	$D_h=(2b\,(a+c))/((a+c)+(2b/\sin\Phi))$		

[*] $d_c=b/\sin(\pi/n)$ [**] $c=a+2b/\tan\Phi$

Table 2. fRe for various cross-sections.

Parallel plate	24	
Circular duct	16	
Rectangular channel	$24\,(1-1.3553\alpha^{*}+1.9467\alpha^{*2}-1.7012\alpha^{*3}+0.9564\alpha^{*4}-0.2537\alpha^{*5})$	
Elliptical channel	$2(1+\alpha^{*2})\,(\pi/E(m))^2$	
Polygonal channel	$8.3880(1+0.3015n-0.0404n^2+0.0024n^3-0.00005n^4)$	
Equilateral Triangular channel	13.3333	
Isosceles Triangular channel	$0\le\alpha^{*}\le 1$	$12(1-0.0115\alpha^{*}+1.7099\alpha^{*2}-4.3394\alpha^{*3}+4.2732\alpha^{*4}-1.5817\alpha^{*5}+0.0599\alpha^{*6})$
	$1\le\alpha^{*}\le\infty$	$12(\alpha^{*3}+0.2595\alpha^{*2}-0.2046\alpha^{*}+0.0552)/\alpha^{*3}$
Right Triangular channel	$12(1+0.27956\alpha^{*}-0.2756\alpha^{*2}+0.0591\alpha^{*3}+0.0622\alpha^{*4}-0.0290\alpha^{*5})$	
Rhombic channel	$0\le\Phi\le 90$	$12(1-0.0231\phi+0.4994\phi^2-0.5002\phi^3+0.2054\phi^4-0.3366\phi^5)$
Trapezoida channel	$f(\alpha^{*},\phi)$	

For circular channel

$$D_{opt}/L = 4.408\ Be^{-1/4} \tag{22a}$$

$$Q^{*}_{\max} = 0.607\ Be^{1/2} \tag{22b}$$

For Rectangular channel

$$b_{opt}/L = \left[0.827\left(1+\alpha^{*}\right)\left(f\,\mathrm{Re}_{Dh}\right)^{3/8}\right]Be^{-1/4} \tag{23a}$$

$$Q^{*}_{\max} = \left[1.370\left(f\,\mathrm{Re}_{Dh}\right)^{-1/4}\right]Be^{1/2} \tag{23b}$$

For elliptical channel

$$b_{opt}/L = \left[0.992\ E(m)\left(f\,\mathrm{Re}_{D_h}\right)^{3/8}\right]Be^{-1/4} \tag{24a}$$

$$Q^{*}_{\max} = \left[1.214\left(f\,\mathrm{Re}_{D_h}\right)^{-1/4}\right]Be^{1/2} \tag{24b}$$

For polygonal channel

$$\frac{b_{opt}}{L} = [1.170n^{1/4}\tan^{3/4}\left(\frac{\pi}{n}\right)\sin^{1/2}\left(\frac{\pi}{n}\right)\left(f\,\mathrm{Re}_{D_h}\right)^{3/8}]Be^{-1/4} \tag{25a}$$

$$Q^{*}_{\max} = [0.685n^{1/2}\sin\left(\frac{\pi}{n}\right)\tan^{-1/2}\left(\frac{\pi}{n}\right)\left(f\,\mathrm{Re}_{D_h}\right)^{-1/4}]\,Be^{1/2} \tag{25b}$$

For equilateral triangular channel

$$b_{opt}/L = 6.559\ Be^{-1/4} \tag{26a}$$

$$Q^{*}_{\max} = 0.717\ Be^{1/2} \tag{26b}$$

For isosceles triangular channel

$$\frac{b_{opt}}{L} = [0.827\left(1+\sqrt{1+4\alpha^{*2}}\right)(f\,\mathrm{Re}_{D_h})^{3/8}]Be^{-1/4} \tag{27a}$$

$$Q^{*}_{\max} = \left[1.370(f\,\mathrm{Re}_{D_h})^{-1/4}\right]Be^{1/2} \tag{27b}$$

For right triangular channel

$$\frac{b_{opt}}{L} = [0.827\left(1+\alpha^{*}+\sqrt{1+\alpha^{*2}}\right)(f\,\mathrm{Re}_{D_h})^{3/8}]\,Be^{-1/4} \tag{28a}$$

$$Q^{*}_{\max} = \left[1.370(f\,\mathrm{Re}_{D_h})^{-1/4}\right]Be^{1/2} \tag{28b}$$

For rhombic channel

$$\frac{b_{opt}}{L} = \left[1.655\ (f\,\mathrm{Re}_{D_h})^{3/8}\right]Be^{-1/4} \tag{29a}$$

$$Q^{*}_{\max} = [1.37(f\,\mathrm{Re}_{D_h})^{-1/4}]Be^{1/2} \tag{29b}$$

For trapezoidal channel

$$\frac{b_{opt}}{L} = [0.827\left(\frac{\sin\phi+\alpha^{*}\cos\phi+\alpha^{*}}{\sin\phi+\alpha^{*}\cos\phi}\right)(f\,\mathrm{Re}_{D_h})^{3/8}]\,Be^{-1/4} \tag{30a}$$

$$Q^{*}_{\max} = [1.37(f\,\mathrm{Re}_{D_h})^{-1/4}]Be^{1/2} \tag{30b}$$

In the above equations α^{*}, Φ, n and $E(m)$, are duct aspect ratio ($\alpha^{*}=b/a$), angle to be used in radians, number of sides of polygon and complete elliptic integral of the second kind in which, $m=1-(\alpha^{*})^2$, respectively.

3. Exact analysis

Yilmaz et al. [5] have developed relations that can plot dimensionless heat transfer per cross sectional area, q^*_A, in terms of dimensionless hydraulic diameter, d^*_h, for various cross sections.

In this analysis the optimal size of channel and maximum heat transfer can be found from two ways. The first is exact solution (ES) considered by Yilmaz et al. [5] and second is the intersection of derived asymptotes from exact analysis [5] in two limiting cases (small and large channels), that hereafter is named exact asymptotic solution (EAS). These asymptotes are as follows:

For small channels, simplifying and considering, $d^*_h \to 0$, we have

$$q^*_A = 1.5625\times 10^{-2}\left(d^{*2}_h / \varphi\right) \tag{31}$$

where

$$\varphi = 1 + \frac{\varphi_\infty - 1}{1 + 0.33 d^{*2.25} / (n-1)} \tag{32}$$

$$\varphi_\infty = (3/8) d^{*2}(3 - d^*) \tag{33}$$

in which d^* and n are dimensionless numbers to describe the shape of the duct cross section

$$d^* = d_h / d_{\max} \tag{34}$$

$$n = p / p_h = A / A_h \tag{35}$$

where d_h, d_{max}, p_h and A_h are the hydraulic diameter, the maximum diameter of the circle which inscribes the actual cross section that is shown in Fig. 4 [5], the periphery and the cross sectional area of the circular duct having the hydraulic diameter d_h, respectively. It can be easily shown that Eq. (31) is identical with Eq. (5).

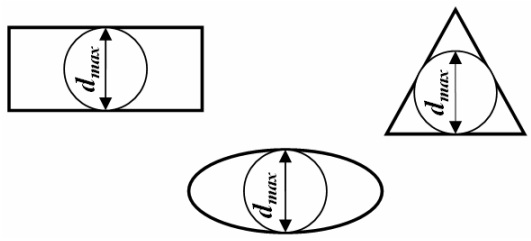

Fig. 4. Definition of d_{max}.

For large channels, $d^*_h \to \infty$, the heat transfer equation is given by

$$\Pr \neq \infty \quad : \quad q^*_A = \frac{1.1306}{f \Pr} d^{*-2/3}_h \tag{36}$$

where

$$f = \left(1 + \frac{0.105}{\Pr + (\sqrt{\Pr}/3)} + \frac{0.0468}{\Pr}\right)^{1/6} \tag{37}$$

The results from Yilmaz et al. [5] were not presented in terms of the Bejan number and required conversion to the notation used in the present work, so the results for both dimensionless heat transfer per cross sectional area and dimensionless hydraulic diameter have been converted to the present notation as follows

$$\frac{D_h Be^{1/4}}{L} = \left(\frac{\Pr}{2}\right)^{1/4} d^*_h \tag{38}$$

$$\frac{Q^*}{Be^{1/2}} = (2\Pr)^{1/2} q^*_A \tag{39}$$

where D_h is the function of channel size, i.e. b and D.

The exact solution of Yilmaz et al. [5] and the above description can be summarized in Fig. 5. The optimal point 1 is achieved from the exact solution (ES) considered by Yilmaz et al. [5] and the optimal point 2 is achieved by exact asymptotic solution (EAS) [5] which is comparable to approximate results from asymptotic analysis in section 2.

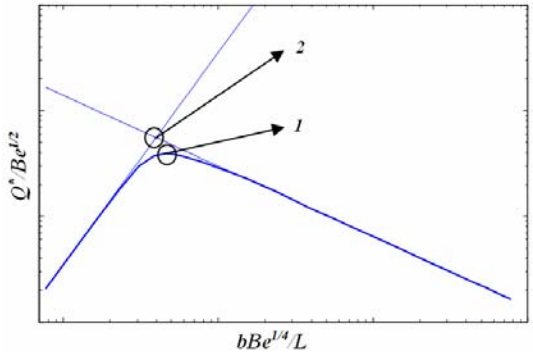

Fig. 5. Exact analysis by Yilmaz et al. [5].

4. Result and discussion

The results for parallel plate channel in Eqs. (21a) and (21b) are exactly the same as those obtained by Bejan and Sciubba [3], and also in Bejan [6, 7].

The maximum dimensionless heat transfer for circular channels is 1.2% lower than the case for parallel plate channels. This difference can be attributed to the fact that tubes cannot fill the volume of space as efficiently as plane channels. This leads to consideration of other geometries which allow for more efficient packing arrangements such as rectangular ducts and triangular ducts.

The results of $b_{opt}Be^{1/4}/L$ and $Q^*_{max}/Be^{1/2}$ for the rectangular and elliptical channels are tabulated as a function of α^* in Table 3.

It is clear that with increasing aspect ratio, maximum dimensionless heat transfer increases slightly. Maximum dimensionless heat transfer in rectangular channels is greater than elliptical channels and is only for full packing the volume of space in the rectangular channels.

The optimal size in polygonal channels can be written in terms of d_i and d_c that are, respectively, inscribed and circumscribed diameters of a regular polygon as follows:

$$d_i = b\cot(\pi/n) \tag{40}$$

$$d_c = b/\sin(\pi/n) \tag{41}$$

Table 3. Results for rectangular and elliptical channel.

α^*	$f\mathrm{Re}_{Dh}$		$b_{opt}Be^{1/4}/L$		$Q^*_{max}/Be^{1/2}$	
	[Rec]	[Elp]	[Rec]	[Elp]	[Rec]	[Elp]
0	24	19.739	2.7258	3.0363	0.6192	0.5761
0.1	21.176	19.314	2.8609	3.0598	0.6388	0.5793
0.2	19.072	18.602	3.0008	3.1195	0.6557	0.584
0.3	17.515	17.896	3.1488	3.2091	0.6698	0.5904
0.4	16.377	17.294	3.3066	3.3247	0.6812	0.5955
0.5	15.557	16.823	3.4752	3.4632	0.6900	0.5996
0.6	14.985	16.479	3.6552	3.6217	0.6965	0.6027
0.7	14.608	16.244	3.8466	3.7977	0.7009	0.6049
0.8	14.382	16.098	4.0492	3.9887	0.7037	0.6063
0.9	14.27	16.022	4.2616	4.1929	0.7051	0.6070
1	14.23	16	4.4812	4.4082	0.7056	0.6072

[Rec] Rectangular [Elp] Elliptical

In the limit of $n\to\infty$ the polygonal channel approaches the circular tube, and therefore for all values of n, the packing is not very efficient. If we consider packing arrangements of polygons arranged according to their circumscribed boundary the reference area becomes $A_r=d_c^2$, like the circular ducts. The results for $b_{opt}Be^{1/4}/L$ and $Q^*_{max}/Be^{1/2}$ as function of n are in Table 4.

The triangle channels are potential candidates for heat sink and heat exchanger designs, because their packing is very complete and efficient. With approximate analysis in section 2 we understand that the triangle channels have the largest dimensionless heat transfer than the above-mentioned channels, for example the $Q^*_{max}/Be^{1/2}$ for equilateral triangular channel is 9.79% and 1.15% greater than the case for parallel plate and square channels, respectively. We will see later which in the exact analysis this increase is likely not realizable in practice but cannot say that this is not a useful shape. The results for $b_{opt}Be^{1/4}/L$ and $Q^*_{max}/Be^{1/2}$ as function of α^* are tabulated in Table 5.

Table 4. Results for polygonal channel.

n	$f\mathrm{Re}_{Dh}$	$b_{opt}Be^{1/4}/L$	$Q^*_{max}/Be^{1/2}$
3	13.435	5.7343	0.40793
4	14.263	3.7715	0.49864
5	14.815	2.9023	0.53855
6	15.167	2.3789	0.55966
7	15.384	2.0209	0.57233
8	15.521	1.7585	0.58059
9	15.624	1.5577	0.58616
10	15.727	1.3996	0.58987
11	15.857	1.2724	0.59212

Table 5. Results for isosceles and right triangular channels.

α^*		$f\mathrm{Re}_{Dh}$		$b_{opt}Be^{1/4}/L$		$Q^*_{max}/Be^{1/2}$	
[Iso]	[Rit]	[Iso]	[Rit]	[Iso]	[Rit]	[Iso]	[Rit]
0	0	12	12	4.20	4.20	0.736	0.736
0.25	0.1	12.61	12.30	4.53	4.46	0.727	0.731
0.5	0.2	13.17	12.54	5.25	4.74	0.719	0.728
0.75	0.3	13.31	12.73	6.12	5.03	0.717	0.725
1	0.5	13.32	12.97	7.07	5.66	0.717	0.722
5	0.7	12.53	13.09	23.60	6.34	0.728	0.720
10	0.8	12.28	13.12	44.58	6.69	0.731	0.720
15	0.9	12.19	13.14	65.59	7.05	0.733	0.719
20	1	12.15	13.15	86.60	7.42	0.734	0.719

[Iso] Isoscele triangular [Rit] Right triangular

Table 6. Results for The trapezoidal channel.

α^*	$f\mathrm{Re}_{Dh}$		$b_{opt}Be^{1/4}/L$		$Q^*_{max}/Be^{1/2}$	
	Φ=30°	Φ=45°	Φ=30°	Φ=45°	Φ=30°	Φ=45°
0	24	24	2.7258	2.7258	0.61916	0.61916
0.5	14.323	15.206	3.4498	3.3799	0.70445	0.69399
1	13.246	13.872	3.7779	3.7886	0.71835	0.7101
2	12.875	13.364	4.0918	4.2518	0.72347	0.71676
8	12.76	13.301	4.4672	4.9308	0.72509	0.71761
1000	12.744	13.153	4.6308	5.2489	0.72532	0.71962
α^*	$f\mathrm{Re}_{Dh}$		$b_{opt}Be^{1/4}/L$		$Q^*_{max}/Be^{1/2}$	
	Φ=60°	Φ=75°	Φ=60°	Φ=75°	Φ=60°	Φ=75°
0	24	24	2.7258	2.7258	0.61916	0.61916
0.5	15.693	15.804	3.3657	3.3943	0.68854	0.68733
1	14.151	14.252	3.8727	4.0724	0.70658	0.70532
2	13.804	14.34	4.5895	5.2764	0.71098	0.70424
8	13.867	14.907	5.8671	8.287	0.71017	0.69744
1000	13.333	13.065	6.5521	10.523	0.71717	0.72082
α^*	$f\mathrm{Re}_{Dh}$		$b_{opt}Be^{1/4}/L$		$Q^*_{max}/Be^{1/2}$	
	Φ=85°		Φ=85°		Φ=85°	
0	24		2.7258		0.61916	
0.5	15.804		3.4407		0.68873	
1	14.252		4.3094		0.70553	
2	14.34		6.1925		0.69619	
8	14.907		13.852		0.67028	
1000	13.065		26.325		0.72921	

In the rhombic channel the maximum dimensionless heat transfer decreases with increasing the angle, as in 90° angle the result of square channel is recovery.

The trapezoidal channel is more efficient because of ability to convert to the other shapes and full packing. The results for $b_{opt}Be^{1/4}/L$ and $Q^*_{max}/Be^{1/2}$ as function of α^* and Φ are tabulated in Table 6.

Further, due to the nature of the approximate method, no absolute conclusion can be made as to which system is better. In any case, to answer this question, one must examine more exact results.

5. Comparison

Primarily, we apply the exact analysis of Yilmaz et al. [5] to the rectangular channel for five different aspect ratios, 0.0; 0.25; 0.5; 0.75; 1.0, as is shown in Fig. 6.

For each aspect ratio there is one curve and two asymptotes; this curve is achieved from exact solution (ES) considered by Yilmaz et al. [5], and the asymptotes are derived from the exact asymptotic solution (EAS) [5].

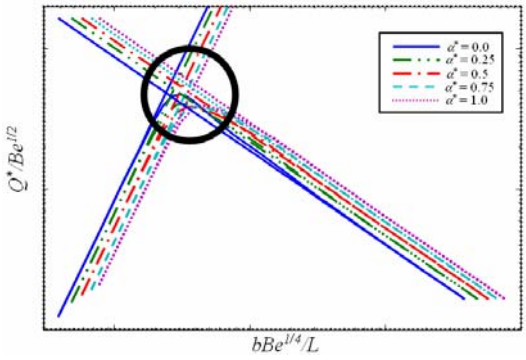

Fig. 6. Exact solutions for the rectangular channel.

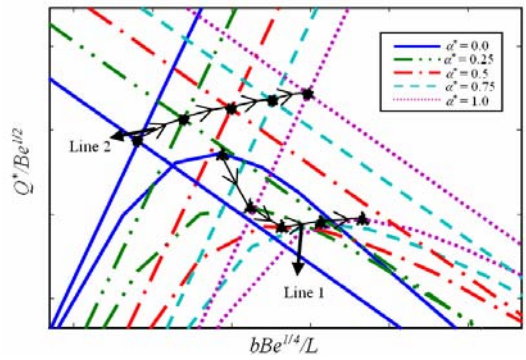

Fig. 7. Variations of optimal point with increasing the aspect ratio for rectangular channel.

Fig. 7 is the magnification of the circle shown in Fig. 6. In Fig. 7, we may realize that with increasing the aspect ratio, in the exact solution of Yilmaz, the maximum dimensionless heat transfer ($Q^*_{max}/Be^{1/2}$) decreases and optimal dimensionless size ($b_{opt}Be^{1/4}/L$) increases as well, (line 1). However, having intersected the two asymptotes at different aspect ratios, it can be concluded that with increasing the aspect ratio both $b_{opt}Be^{1/4}/L$ and $Q^*_{max}/Be^{1/2}$ increase (line 2).

Note that the intersection of asymptotes at different aspect ratios is the locus of optimal points. This contradiction in results of ES and EAS is due to the nature of the method of asymptotes. In these cases the actual heat transfer curve is lower for the square, while the intersection point of the asymptotes is higher for the square, when compared with the parallel plate geometry.

The present work namely, the approximate asymptotic solution (AAS), described in section 2, is

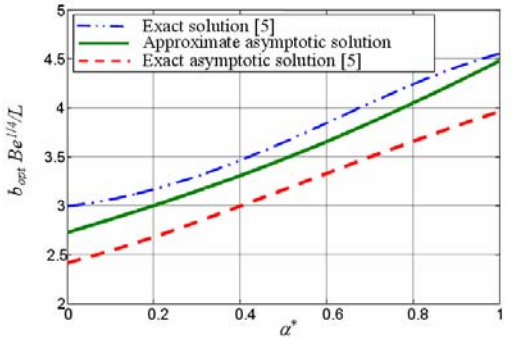

Fig. 8. Variations of optimal dimensionless size with the aspect ratio for rectangular channel.

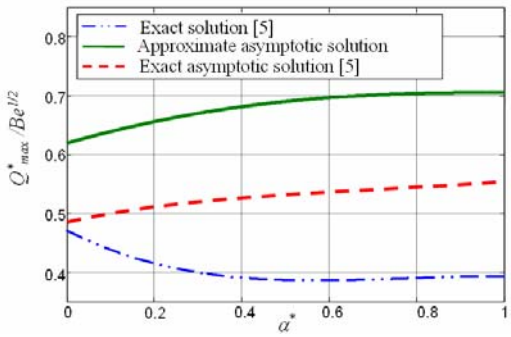

Fig. 9. Variation of maximum dimensionless heat transfer with the aspect ratio for rectangular channel.

in excellent agreement with the exact asymptotic solution for various cross sections. This issue can be shown in the following figures.

In Figs. 8 and 9 the optimal dimensionless size and maximum dimensionless heat transfer curves in terms of aspect ratio, for rectangular channel, have been plotted.

In Figs. 10 and 11, the influence of aspect ratio on $b_{opt}Be^{1/4}/L$ and $Q^*_{max}/Be^{1/2}$ for elliptical (a) and isosceles triangular (b) channels has been shown.

6. Summary and conclusion

An approximate expression for the optimal duct shape is being developed for several ducts shapes. Comparison of the approximate results with exact results from the literature shows excellent agreement for the optimal duct dimensions. Maximum dimensionless heat transfer per unit volume also agrees well with the exact results; however, more accurate results should be computed by using conventional methods once the optimal geometry is found with the present approach.

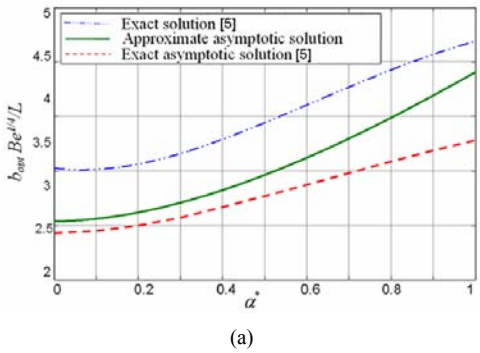

(a)

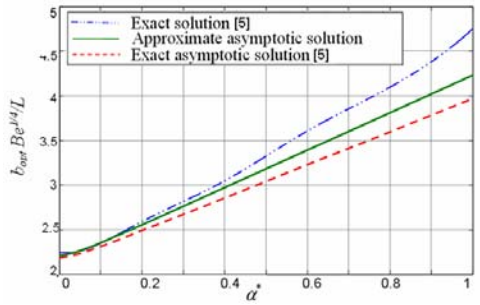

(b)

Fig. 10. Variation of optimal dimensionless size with aspect ratio for elliptical (a), and isosceles triangular (b) channels.

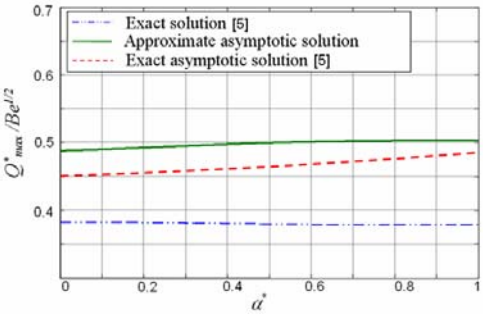

(a)

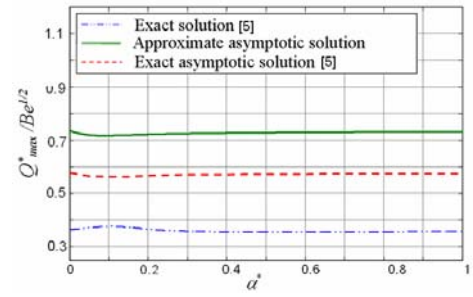

(b)

Fig. 11. Variation of maximum dimensionless heat transfer with aspect ratio for elliptical (a), and isosceles triangular (b) channels.

Nomenclature

A : Flow area, m^2
A_r : Reference cross sectional area, m^2
a,b : Major and minor axes of ellipse or rectangle, m
Be : Bejan number, $\equiv \Delta PL^2/\mu\alpha$
C_p : Specific heat, J/kgK
D : Diameter of circular duct, m
D_h : Hydraulic diameter, $\equiv 4A/P$
$E(m)$: Complete elliptic integral of second kind
f : Friction factor
k : Thermal conductivity, W/mK
h : Convective heat transfer coefficient, W/m^2K
H : Height, m
L : Duct length, m
$\dot{m}$: Mass flow rate, kg/s
n : Number of sides of polygon, number of channels or ducts
P : Pressure, N/m^2
p : Perimeter, m
Pr : Prandtl number, $\equiv \upsilon/\alpha$
Q : Heat transfer rate, W
q : Heat transfer per unit volume, $\equiv Q/HWL$
Q^* : Dimensionless Q
Re : Reynolds number
T_i : Fluid inlet temperature, K
T_w : Temperature at wall, K
U : Average velocity, m/s
U_∞ : Free stream velocity, m/s
V : Volume, m^3
W : Width, m

Greek symbols

α : Thermal diffusivity, m^2/s
α^* : Aspect ratio, $\equiv b/a$
μ : Dynamic viscosity, Ns/m^2
υ : Kinematic viscosity, m^2/s
ρ : Density, kg/m^3
τ : Wall shear stress, N/m^2
φ : Shape factor for pressure loss
Φ : Angle, Radian

Superscripts and Subscripts

* : Dimensional
c : Circumscribed
D_h : Based upon the hydraulic diameter
f : Fluid
i : Inscribed
l : Large
m : Maximum
s : Small

Abbreviations

AAS : Approximate Asymptotic Solution
EAS : Exact Asymptotic Solution
ES : Exact Solution

References

[1] D. B. Tuckerman and R. F. Pease, High-performance heat sinking for VLSI, *IEEE Electron Device Lett.*, 5 (1981) 126-129.
[2] M. Bahrami, M. M. Yavanovich and J. R. Culham, Pressure drop of fully developed laminar flow in microchannels of arbitrary cross-section, *Transactions of the ASME,* 128 (2006).
[3] A. Bejan and E. Sciubba, The optimal spacing of parallel plates cooled by forced convection, *Int. J. Heat Mass Transfer*, vol. 35 (1992) 3259-3264.
[4] S. Petrescu, Comments on the optimal spacing of parallel plates cooled by forced convection, *Int. J. Heat Mass Transfer,* 37 (1994) 1283.
[5] A. Yilmaz, O. Buyukalaca and T. Yilmaz, Optimum shape and dimensions of ducts for convective heat transfer in laminar flow at constant wall temperature, *Int. J. Heat Mass Transfer,* 43 (2000) 767-775.
[6] A. Bejan, Shape and structure, from engineering to nature, *Cambridge University Press, Cambridge, K,* 2000 35-37.
[7] A. Bejan, Convection heat transfer, *Wiley, New York, NY*, 2004 136-141.
[8] R. K. Shah and A. L. London, Laminar flow forced convection in ducts, *Academic Press, NY*, 1978 78-283.
[9] R. K. Shah and M. S. Bhatti, Laminar convective heat transfer in ducts, in S. Kakac, R. S. Shah and W. Aung, Handbook of single-phase convective heat transfer. *Wiley, New York, NY,* (1987).
[10] R. K. Shah, Laminar flow friction and forced convection heat transfer in ducts of arbitrary geometry, *Int. J. Heat Mass Transfer*, 18 (1975) 849-862.

Omid Asgari received his B.S. in Mechanical Engineering from Karaj University, IRAN, in 2005. He then received his M.S. degree from Sharif university of Technology in 2007. Mr. Asgari is currently a PHD student at the School of Mechanical Engineering at Sharif University of Technology in Tehran, Iran. His research interests include heat transfer, thermodynamics, combustion, micro fluid and new energies such as geothermal energy.